

## Comparative Rheology of Graphene-PS and Graphene-PMMA nanocomposites



### Physics

**KEYWORDS :** Polymer nanocomposites, graphene, polystyrene, PMMA, rheology

**Manasi Singhi**

Department of Chemistry, Ambedkar Institute of Advanced Communication Technologies and Research, Geeta Colony, New Delhi, India

\* **M. Fahim**

Department of Physics, Zakir Husain Delhi College, University of Delhi, New Delhi- 110002, India. \* Corresponding author

### ABSTRACT

*Graphene filled polymer nanocomposites have attracted a keen interest in the recent past owing to their better structural, morphological, electrical and rheological properties compared to the base polymeric matrices. In this paper, rheological properties of two commercially important polymers viz. PMMA and PS have been investigated and compared firstly, to study the influence of graphene and secondly, to find an optimum percentage of graphene required for best possible rheological properties in both the systems. Frequency sweep measurements were done to study the linear viscoelastic properties of both the systems at a fixed strain. A noticeable nonlinear region at higher strain amplitudes was observed which was attributed to the formation of more strain-sensitive rigid network-like structures which rupture at higher strain amplitudes, leading to a narrower region of linear viscoelasticity. Nanocomposites containing higher graphene percentage were predominated by network like structures compared to the pure polystyrene. Cole-Cole plot of Polystyrene-Graphene nanocomposites showed a deviation from a semi-circular shape with increasing graphene concentration. It was attributed to the fact that at low graphene concentration, polymer-filler interaction is high due to proper exfoliation of graphene into polymer matrix. With increasing nano filler percentage, exfoliation becomes difficult and filler-filler interaction predominated over polymer-filler interaction. It was also observed that crossover frequencies decreased and characteristic relaxation time increased with increasing graphene content in graphene-PS system.*

### 1.0 Introduction

Studies on the rheological properties of polymer nanocomposites assume greater significance owing to the former's close relation to the microstructure of nanocomposites, dispersion of nanofillers and the interactions between nanofillers and polymer microstructure. Numerous polymer nanocomposites have been characterized for their rheological behavior in order to understand the processing operations [1-8]. For instance, non-terminal low-frequency rheological behavior has been observed in the case of nanocomposites containing layered silicates [1]. At low oscillation frequencies, a transition to solid like response for PEO/silica nanocomposites has been observed [2]. Similar, non-terminal solidlike rheological behavior has been observed for polymer nanocomposites containing carbon fibers and carbon nanotubes [3,4]. This non-terminal solidlike rheological behavior results from a filler network formed in the nanocomposites. In the case of SWNT/PMMA nanocomposites, a difference in rheological threshold and electrical percolation threshold was observed. It was attributed to the smaller filler-filler distance required for electrical conductivity as compared to that required to impede polymer mobility [5]. Similarly, in the case of polycarbonate/TEGO composite, the storage modulus plateau obtained in linear viscoelastic rheology measurements indicated a rheological percolation due to formation of a solid-like' elastic network of filler [9]. This percolation threshold gives a rough estimation of dispersion of filler particles [10-11]. The onset of rheological percolation has been studied by measuring dynamic moduli of polymer nanocomposites obtained using dynamic mechanical analysis (DMA) temperature scans [12-15]. It has been reported that the thermal annealing beyond  $T_g$  of polymer promotes randomization of filler orientations and lowers the rheological percolation threshold [11]. The viscosities of composite solutions have also been studied and compared. For instance, polymers containing graphene nanoplatelets (GNP) fillers showed lower viscosities compared to CNTs [16]. It was attributed to the fact that at sufficiently high loadings, entanglement of CNTs in the matrix might have led to large viscosity increases. However, in the case of platelets, the viscosity increase was reduced since platelets can more easily slide past one another [17]. The solution viscosities of CMG/epoxy composites have been reported to increase substantially with loading of filler [18]. This increase in viscosity can be moderated if

the compatibility of filler with polymer matrix can be improved using functionalization of fillers [14]. In the case of melt compounded PS/functionalized graphene sheets (FGS) composites that were subjected to long-term thermal curing it was observed that composites gained enhanced viscoelasticity probably due to particle percolation. Aging also reduced the yield strain for FGS networks [14a].

In this paper, two polymeric systems, graphene filled Polystyrene and graphene filled PMMA were chosen for investigating their respective rheological behaviour and compare their performance. Both the systems were prepared and tested in identical test conditions. The objective of this work was to establish a relation between the microstructure of polymers and their interaction with the nanofiller. Another aim of this work was to study the influence of graphene on the microstructure and properties of these polymers.

### 2.0 Experimental

Styrene monomer (Density = 0.906g/ml at 25°C, molecular weight = 104.15g/mol, melting point = -31°C, boiling point = 145-146°C and purity  $\geq$  99%) was obtained from Sigma Aldrich, Germany. Benzoyl peroxide (Melting point = 54°C) was obtained from Sigma Aldrich, Germany. This was formulated specially for use with Histoacryl and LR white acrylic resin. OH-Graphene Nanopowder (Purity = 99.5%, Layer Flake = 4-6 (50-80%), Surface Area  $\geq$  250m<sup>2</sup>/g, Thickness = 2-4nm, Lateral Size = 1-10µm, pH = 6-7, Ash = <0.5%, Morphology = Flaky) was obtained from Nanoshel LLC. In-situ polymerization of Styrene monomer was carried out in test tubes with the help of ultra-sonication under suitable condition. Exact amount of graphene was taken in dry test tubes and then it was sonicated for 5 minutes in dry condition. 10g of Styrene monomer and 0.1g of BPO initiator were added to the test tubes. Nitrogen was purged for 1 minute in every test tube to create an inert atmosphere. Test tubes were plugged tightly with cotton and sonicated for 15 minutes at room temperature. Now, these systems were slowly heated to 80°C and sonicated for total 4 hours until the monomer system became viscous and graphene got entrapped into the polymer chains. After 4 hours, sonication was stopped and systems were heated for another 20 hours to complete the in-situ polymerization under nitrogen atmosphere. After 24 hours polymeric lumps were formed inside the test tube. Test tubes were broken to

take the polymeric lumps out. Then these polymer lumps were crushed at 20,000 lb pressure in compression moulding machine without heating. Thus, micro cracks developed inside the lump-sand then they were granulated with the help of polymer cutter. Granules were dried at 80°C under vacuum for 24 hours to remove low molecular weight components. After that, granules were compression moulded to make samples at 180°C and at 15,000 lb pressure. Samples were slowly cooled to 65°C and then they were ejected from the mould. Total eight different sample compositions were prepared by varying the weight percentage of graphene as shown in Table1a. Same procedure was used to prepare graphene filled PMMA nanocomposites (Table 1b) as described elsewhere [19]

### 3. 0 Results and Discussion

#### 3.1DSC Analysis

Differential scanning calorimetry (DSC) of the nanocomposites was done by using TA Instruments DSC Q 200 machine. The first heating rate was 10°C/min, the cooling rate was 10°C/min and also the second heating rate was 10°C/min. Nanocomposite samples were heated from room temperature to 180°C. The second heating cycle was taken to avoid any thermal stress history. The glass transition temperatures ( $T_g$ ) of the resulting nanocomposite samples were studied by DSC analysis by observing the base line shift. It is observed that  $T_g$  of the Polystyrene-Graphene nanocomposites remains almost in same range with increase in the weight percentage of graphene. However,  $T_g$  slightly increases when graphene is incorporated in the pure polystyrene matrix. This increase in  $T_g$  can be described by the retardation of molecular motion due to interaction with the high surface area of graphene nanopowder [20].

#### 3.2 TGA & DTGA Analysis

Thermo Gravimetric analysis (TGA) and differential thermo gravimetric analysis (DTGA) of the nanocomposites were done by using Perkin Elmer Pyris 6 TGA machine. The nanocomposite samples were heated from 50°C to 750°C with a heating rate of 20°C/min in nitrogen atmosphere and at a constant nitrogen flow rate. Thermal stability of the resulting nanocomposite samples were studied by TGA and DTGA analysis by observing the changes in onset of degradation temperature ( $T_{onset}$ ), inflection temperature and end of degradation temperature ( $T_{end}$ ). TGA and DTGA analysis are summarised in Table2. TGA results show that the onset degradation temperature and thermal stability of Polystyrene-Graphene nanocomposites increases due to incorporation of graphene. As the graphene weight percentage increases, onset of degradation temperature increases and thus the thermal stability of the nanocomposites also increases. It is also observed that end of degradation temperature also shows an increasing pattern for all the nanocomposites with increase in graphene percentage. This is believed to result from the intercalation of polystyrene into the lamellae of graphite. From the DTGA data, it is observed that inflection point temperature also increases with increase in graphene weight percentage. Therefore by incorporating graphene nanopowder into pure polystyrene matrix, a considerable increase in thermal stability can be achieved [20-21].

#### 3.3 Rheological Studies

Figure1a shows the plots of elastic modulus dependence of strain for pure Polystyrene (PSG000) and PSG250 at 200°C at a frequency of 1 Hz while Fig. 1b shows the plots of elastic modulus dependence of strain for pure PMMA (PG000) and PG250 at 180°C at a frequency of 1 Hz. It is evident that the regions of linear viscoelastic behaviour for pure Polystyrene (PSG000) as well as pure PMMA (PG000) are wider than that of their respective composites due to the presence of graphene in composites. It is interesting to note that the linear viscoelastic regions (LVR) for PSG000 extend to a strain of 1 and that for PSG250 is about 0.1 under the testing conditions. After those certain strains, the

curves start to fall. Therefore, frequencysweep, to study the linear viscoelastic properties of Polystyrene-Graphene nanocomposites were conducted at a fixed strain of 0.01 at 200°C. However, in the case of PMMA the linear viscoelastic regions extended to a strain of 0.1 and that for PG250 was about 0.01 under the testing conditions. After those certain strains the curves start to fall. Therefore, frequency sweep, to study the linear viscoelastic properties of PMMA/Graphene nanocomposites were conducted at a fixed strain of 0.005 at 180°C.

In both the PS-graphene and PMMA-graphene systems (pure as well as composite), it was observed that elastic modulus exhibits a linear region at low strain amplitudes. However, a noticeable nonlinear region at higher strain amplitudes can be observed which is called Payne effect. This behaviour could be attributed to the formation of more strain-sensitive rigid network-like structures which rupture at higher strain amplitudes, leading to a narrower region of linear viscoelasticity. And in higher graphene percentage network like structures are more which breaks at a lower strain than compared to the pure polymer. Therefore, linear viscoelastic region (LVR) of composites is shorter than that of pure polymer.

#### 3.3.1 Linear viscoelastic region of PS-Graphene system

Figures 2(a-c) show the variation of storage modulus ( $G'$ ), loss modulus ( $G''$ ) and dissipation factor ( $\tan \delta$ ) against frequency respectively of Polystyrene-graphene system. Comparison of the linear viscoelastic response of the materials shows the significant effect of the graphene loading with frequency. As the graphene percentage increases, storage modulus and loss modulus of nanocomposites compared with pure Polystyrene shows a monotonic increase. The reason for the increase of storage modulus and loss modulus might arise from the confinement of polymer chains within the graphene layers. With increasing graphene loading nanocomposites show non-terminal behavior i.e. elastic modulus and viscous modulus become nearly independent of frequency which is consistent with the transition from liquid like to pseudo-solid like behavior of polymer melt with increasing graphene loading due to formation of polymer-graphene network. Due to incorporation of graphene nano filler, increase of storage modulus ( $G'$ ) is expected due to the additivity principle of modulus and it increases a considerable amount in a graphene percentage as low as 0.25 wt.%. In low percentage of filler the plot of PSG025 follows the same nature as that of pure Polystyrene (PSG000). But as the filler percentage increases, the nature of the curve changes and they increase slowly throughout the entire frequency range. In case of loss modulus ( $G''$ ), as nanofiller percentage increases, the viscous part increases and consequently the loss modulus also increases. From the curves it is noticeable that loss modulus increases at higher frequencies. In Fig. 3, it is observed that complex viscosity of nanocomposites decreases with increase in frequency. As with increase in graphene content the viscous part increases in the nanocomposites, viscosity of the nanocomposites are higher than that of pure Polystyrene (PSG000) and it remains higher in the complete frequency range though the curves follow same decreasing nature with frequency [5,22,23]. At lower frequency the loss modulus value is higher than that of storage modulus, but at high frequency the opposite case is observed and the storage modulus value becomes higher than that of loss modulus, which is associated with a cross-over frequency for each composition. That means there is a transition from liquid-like behaviour to pseudo solid-like behaviour of the polymer melt. Figure 4 shows the crossover points from elastic and viscous modulus when they are plotted against frequency of Polystyrene-Graphene nanocomposites. The crossover frequency values and corresponding characteristic relaxation time (considering Maxwell Model), obtained from Fig. 4, are given in Table 3. Crossover frequency is defined as the frequency at which elastic modulus of the polymer melt become equal to viscous modulus. It is observed that

crossover frequency of different compositions of resulting nanocomposites decreases with increasing graphene loading because of pseudo-solid like behaviour of polymer melt. From Table 3, it is prominent that crossover frequencies decreases and characteristic relaxation time increases with increasing graphene content. Relaxation time represents the time required by the polymer molecules to relax completely during processing. It is a very important parameter as it indicates whether there is any in-built stress in the sample or not. If processing time is greater than relaxation time then the polymer molecules get sufficient time for relaxation and the resulting samples contains no in-built stress. It is observed that pure polystyrene has least relaxation time but when graphene is incorporated then it increases. Incorporation of graphene put restriction on molecular mobility and consequently polymer molecules take longer time to relax. So it is expected that relaxation time will increase with increase in graphene loading. In PSG250, as graphene loading is highest, relaxation time is also much highest among other compositions. In this project work, samples are made by compression moulding process which provides very long processing and cooling time as compared to other conventional processing techniques. As cooling time is much longer than that of the characteristic relaxation time of the samples, it is obvious that the resulting samples are completely relaxed and no in-built stresses are there in the samples. Figure 5 shows the Cole-Cole viscosity representation of the resulting Polystyrene-Graphene nanocomposites. This Cole-Cole viscosity representation is analysed to know the miscibility and interaction of graphene in polystyrene matrix. The real part ( $\eta'$ ) and imaginary part ( $\eta''$ ) of complex viscosity are calculated according to the following equations 1 and 2 respectively:

$$\eta' = G'' / \omega \text{ ----- (1)}$$

$$\eta'' = G' / \omega \text{ ----- (2)}$$

The curves proximity to a semi-circular shape indicates higher miscibility or interaction and the deviation from the semi-circular shape indicates the reduction in interaction of graphene with polystyrene matrix. Here, it is observed that with increasing graphene percentage the curves deviate from semi-circular shape. At low graphene concentration, polymer-filler interaction is high due to proper exfoliation of graphene into polymer matrix. But, as the nano filler percentage increases exfoliation becomes difficult and filler-filler interaction predominates over polymer-filler interaction and consequently a deviation from the semi-circular shape is observed in the Cole-Cole plot. It also indicates the transition from liquid-like behaviour to pseudo solid-like behaviour of the polymer melt. In PSG250, the curve is almost a straight line which indicates that maximum filler-filler interaction has occurred in this composition [24].

**3.3.2 Linear viscoelastic region of PS-Graphene system**

Figures 6 (a-c) show the variation of storage modulus ( $G'$ ), loss modulus ( $G''$ ) and dissipation factor ( $\tan \delta$ ) against frequency respectively of PMMA-graphene system. Comparison of the linear viscoelastic response of the materials shows the significant effect of the Graphene loading with frequency. As the Graphene percentage increases, storage modulus and loss modulus of nanocomposites compared with pure PMMA shows a monotonic increase. The reason for the increase of storage modulus and loss modulus might arise from the confinement of polymer chains within the Graphene layers. Due to incorporation of nano filler, increase of storage modulus ( $G'$ ) is expected due to the additive principle of modulus and it increases a considerable amount in a Graphene percentage as low as 0.25 wt.%. In low percentage of filler the plot of PG025 follows the same nature as that of pure PMMA (PG000). But as the filler percentage increases the nature of the curve changes and they increases slowly throughout the entire frequency range. In case of loss modulus ( $G''$ ), as nano filler percentage increases, the viscous part increases and

consequently the loss modulus also increases. From the curves it is noticeable that loss modulus increases at higher frequencies. In Fig. 7 it is observed that complex viscosity of nanocomposites decreases with increase in frequency. As with increase in Graphene content the viscous part increases in the nanocomposites, viscosity of the nanocomposites are higher than that of pure PMMA (PG000) and it remains higher in the complete frequency range though the curves follow same decreasing nature with frequency [27].

**3.0 Conclusions**

Non-functionalised graphene was incorporated in two polymeric matrices namely polystyrene and PMMA via in-situ polymerization to form nanocomposites. The microstructure of these nanocomposites was studied and compared using rheological characterization. It was observed that in both the polymeric systems, with increasing graphene loading, nanocomposites showed non-terminal behavior i.e. elastic modulus and viscous modulus become nearly independent of frequency indicating transition from liquid like to pseudo-solid like behavior of polymer melt due to formation of polymer-graphene network. Graphene filled PS nanocomposites showed better rheological properties than PMMA due to better dispersion and low viscosity composite solution obtained in PS based system. It was also observed that relaxation time was higher for nanocomposite than pure polystyrene because graphene fillers restricted the molecular mobility which rendered difficult the relaxation of polymer molecules. Since samples were compression moulded which provided very long processing and cooling time, the composites were completely relaxed with no in-built stresses. The relaxation time was found to be higher in the case of polymer nanocomposites compared to pure polymers because of pseudo-solid like behaviour of polymer melt due to the presence of graphene.

**Table 1a Polystyrene-Graphene nanocomposites**

Sample Name	Polystyrene (wt.%)	BPO (wt.%)	Graphene (wt.%)
PSG000	100	1.00	0.00
PSG025	100	1.00	0.25
PSG050	100	1.00	0.50
PSG075	100	1.00	0.75
PSG100	100	1.00	1.00
PSG150	100	1.00	1.50
PSG200	100	1.00	2.00
PSG250	100	1.00	2.50

**Table 1b PMMA-Graphene nanocomposites**

Sample Name	PMMA (wt.%)	BPO (wt.%)	Graphene (wt.%)
PG000	100	1.00	0.00
PG025	100	1.00	0.25
PG050	100	1.00	0.50
PG075	100	1.00	0.75
PG100	100	1.00	1.00
PG125	100	1.00	1.25
PG150	100	1.00	1.50
PG175	100	1.00	1.75
PG200	100	1.00	2.00
PG250	100	1.00	2.50

**Table 2 TGA and DTGA results of the Polystyrene-Graphene nanocomposites**

Sample Name	TGA Data		DTGA Data
	Onset of Degradation T <sub>Onset</sub> (°C)	End of Degradation T <sub>End</sub> (°C)	Point of Inflection (°C)
PSG000	397.91	429.34	416.70
PSG025	400.47	433.04	422.73
PSG050	403.28	436.23	426.62
PSG075	404.40	435.84	424.60
PSG100	403.19	432.36	420.04
PSG150	401.15	432.76	420.60
PSG200	403.17	434.52	423.05
PSG250	402.90	436.05	424.82

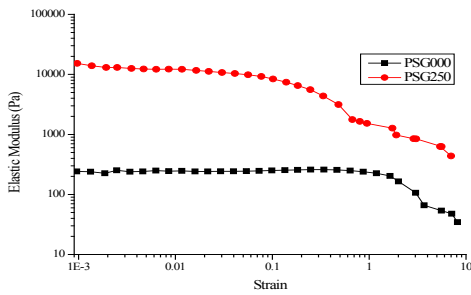


**Figure 1a: Strain sweep test of pure Polystyrene (PSG000) and PSG250**

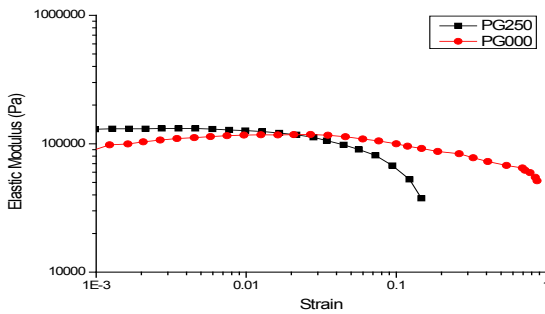


**Figure 1b: Strain sweep test of PMMA (PG000) and PG250**

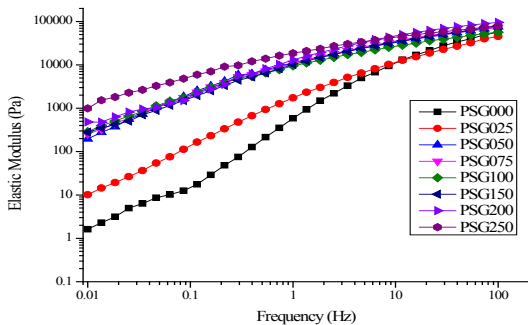


**Figure 2a Plot of Elastic modulus (G') vs Frequency of Polystyrene-Graphene nanocomposites**

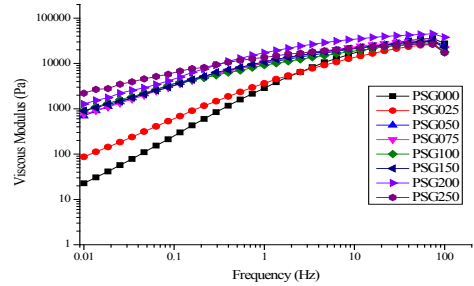


**Figure 2b: Plot of Viscous modulus (G'') vs Frequency of Polystyrene-Graphene nanocomposites**

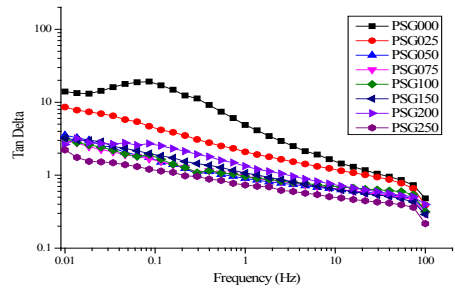


**Figure 2c: Plot of Dissipation Factor (tan δ) vs Frequency of Polystyrene-Graphene nanocomposites**

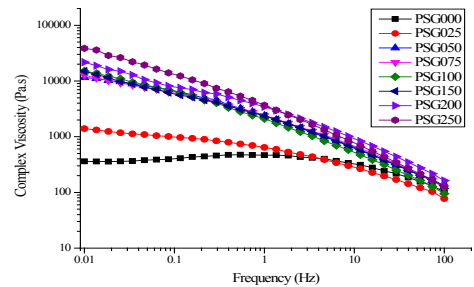


**Figure 3: Plot of Complex Viscosity vs Frequency of Polystyrene-Graphene nanocomposites**

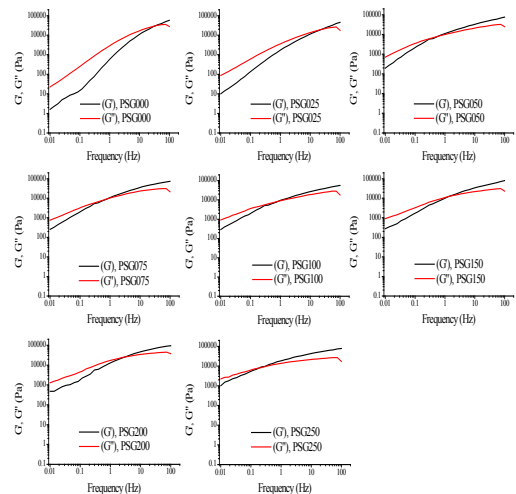


**Figure 4: Crossover points from Elastic and Viscous Modulus vs. Frequency of Polystyrene-Graphene nanocomposites**

**Table 3: Variation of crossover frequencies and characteristic relaxation times for Polystyrene-Graphene nanocomposites**

Relaxation Time $\lambda$ (s)	Crossover Freq. ( $s^{-1}$ )	Sample Number
0.027	36.902	PSG000
0.040	24.708	PSG025
1.513	0.6608	PSG050
1.133	0.8827	PSG075
1.173	0.8523	PSG100
0.693	1.4423	PSG150
0.319	3.1264	PSG200
5.426	0.1843	PSG250

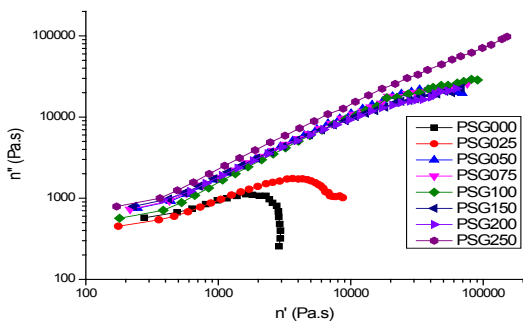


**Figure 5: Cole-Cole plot of Polystyrene-Graphene nanocomposites**

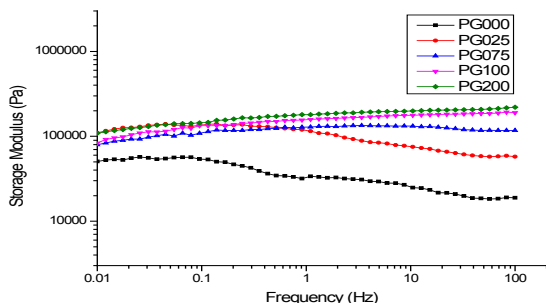


**Figure 6a: Plot of Storage modulus ( $G'$ ) vs Frequency**

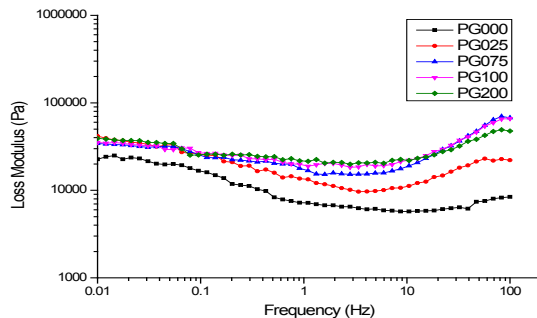


**Figure 6b: Plot of Loss modulus ( $G''$ ) vs Frequency**

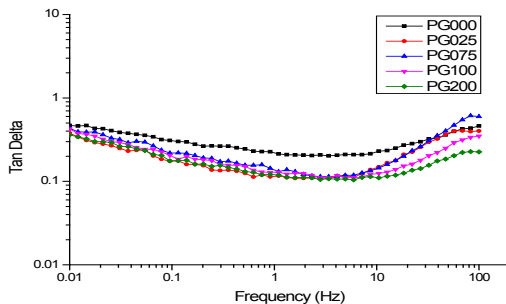


**Figure 6c: Plot of Dissipation Factor ( $\tan \delta$ ) vs Frequency**

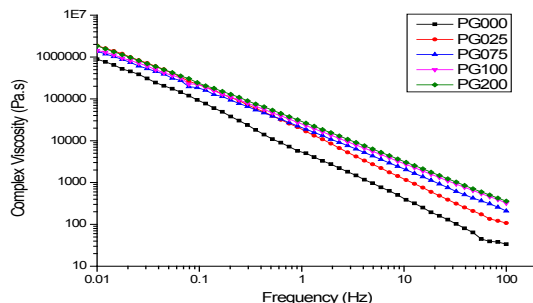


**Figure 7: Plot of Complex Viscosity vs Frequency**

**REFERENCE**

Krishnamoorti, R.; Giannelis, E. P. *Macromolecules* 1997, 30, 4097-4102. | [2] Zhang, Q.; Archer, L. A. *Langmuir* 2002, 18, 10435-10442. | [3] Lozano, K.; Bonilla-Rios, J.; Barrera, E. V. J. *Appl. Polym. Sci.* 2000, 80, 1162-1172. | [4] Potschke, P.; Fornes, T. D.; Paul, D. R. *Polymer* 2002, 43, 3247-3255. | [5] Fangming Du, Robert C. Scogna, Wei Zhou, Stijn Brand, John E. Fischer, and Karen I. Winey, *Macromolecules*, 2004, 37, 9048-9055 | [6] Solomon MJ, Almusallam AS, Seefeldt KF, Somwangthanaroj A, Varadan P. *Macromolecules* 2001, 34, 1864-72. | [7] Wagener R, Reisinger T J G. *Polymer* 2003, 44, 7513-8. | [8] Zhang Q, Fang F, Zhao X, Li Y, Zhu M, Chen D. *J Phys Chem B* 2008, 112, 12606-11. | [9] Vermant J, Ceccia S, Dolgovskij MK, Maffettone PL, Macosko CW. *J Rheol* 2007, 51, 429-50. | [10] Kim H, Macosko CW. *Macromolecules* 2008, 41, 3317-27. | [11] Kim H, Macosko CW. *Polymer* 2009, 50, 3797-809 | [12] Ganguli S, Roy AK, Anderson DP. *Carbon*, 2008, 46, 806-17. | [13] Ramanathan T, Stankovich S, Dikin DA, Liu H, Shen H, Nguyen ST, et al. *J Polym Sci Part B Polym Phys* 2007, 45, 2097-112. | [14] Ansari S, Giannelis EP. *J Polym Sci Part B Polym Phys*, 2009, 47, 888-97 | [14a] Hyunwoo Kim, Ph.D Thesis "Processing, Morphology and Properties of Graphene Reinforced Polymer Nanocomposites", University of Minnesota, September 2009 | [15] Pramoda KP, Linh NTT, Tang PS, Tjiu WC, Goh SH, He CB. *Compos Sci Technol*, 2009, 578-83. | [16] Yu A, Ramesh P, Itkis ME, Bekyarova E, Haddon RC. *J Phys Chem C* 2007, 111, 7565-9. | [17] Jang BZ, Zhamu A. *J Mater Sci* 2008, 43, 5092-101 | [18] Fang M, Zhang Z, Li J, Zhang H, Lu H, Yang Y. *J Mater Chem* 2010, 20, 9635-43. | [19] Soumyajit Basu, Manasi Singhi, Bhabani K. Satapathy, M. Fahim, *Polymer Composites*, 2013, 34(12), 2082-2093. | [20] Yiu-Wing Mai and Zhong-Zhen Yu, (Eds) *Polymer nanocomposites*, Woodhead Publishing and Maney Publishing on behalf of The Institute of Materials, Minerals & Mining CRC Press Boca Raton Boston New York Washington, DC (2006) | [21] Fawn M. Uhl, Charles A. Wilkie, *Polymer Degradation and Stability* 76 (2002) 111-122 | [22] Caroline McClory, Tony McNally, Mark Baxendale, Petra Pötschke, Werner Blau, Manuel Ruether, *European Polymer Journal* 46 (2010) 854-868 | [23] M. Annala, M. Lahelin, J. Seppälä, *EXPRESS Polymer Letters*, 6(10) (2012) 814-825 (available online at [www.expresspolymlett.com](http://www.expresspolymlett.com)) | [24] I Ivanov, S. Muke, N Kao, S.N. Bhattacharya, *Polymer* 42 (2001) 9809-9817 |